

Article

Physical and Rheological Characteristics of Sediment for Nautical Depth Assessment in Bushehr Port and Its Access Channel

Farzin Samsami ^{1,*} , Seyyed Abbas Haghshenas ² and Mohsen Soltanpour ³ ¹ Civil Engineering Department, West Tehran Branch, Islamic Azad University, Tehran 1461988631, Iran² Institute of Geophysics, University of Tehran, Tehran 1435944411, Iran³ Civil Engineering Department, K. N. Toosi University of Technology, Tehran 1996715433, Iran

* Correspondence: samsami@wtiau.ac.ir

Abstract: Sedimentation in ports and waterways covered with fine deposits is a significant challenge in harbor management. The top layer of the bed in such areas typically consists of fluid mud, for which dredging is complicated and less efficient. The goal of this paper is to investigate physical and rheological characteristics of sediment for nautical depth assessment in Bushehr Port and its access channel. In this study the fluid mud layer was detected by hydrographic surveys with a dual-frequency echo sounder. Moreover, sediment properties in various parts of the channel and port were analyzed through a comprehensive sediment sampling in the field and complementary laboratory studies, including sediment grain-size analysis and distribution, carbonate and organic matter content, rheometry, and consolidation and settling tests. It was found that water contents and concentration, and clay-size fractions are the most important factors in rheological characteristics of sediment in the study area. The results indicated that the clay-size fraction in the surficial bed was between 18 and 31%, which categorized it as fine and cohesive sediment. In terms of mineralogy, the sediment was mostly carbonate mud with carbonate content between 52.9 and 57.2%. The results showed that the sediment concentration and yield stress in most samples were lower than 1030 kg/m³ and 123 Pascals, respectively. Based on the hydrographic surveys and obtained sediment characteristics, it is concluded that the nautical bottom approach can be practically implemented in the Bushehr Port and its access channel.

Keywords: fine and cohesive sediment; fluid mud; rheology; nautical bottom; dual-frequency echo sounding; Bushehr Port



Citation: Samsami, F.; Haghshenas, S.A.; Soltanpour, M. Physical and Rheological Characteristics of Sediment for Nautical Depth Assessment in Bushehr Port and Its Access Channel. *Water* **2022**, *14*, 4116. <https://doi.org/10.3390/w14244116>

Academic Editor: Bommanna Krishnappan

Received: 29 October 2022

Accepted: 12 December 2022

Published: 16 December 2022

Publisher's Note: MDPI stays neutral with regard to jurisdictional claims in published maps and institutional affiliations.



Copyright: © 2022 by the authors. Licensee MDPI, Basel, Switzerland. This article is an open access article distributed under the terms and conditions of the Creative Commons Attribution (CC BY) license (<https://creativecommons.org/licenses/by/4.0/>).

1. Introduction

Due to sedimentation in ports and navigation channels covered with fine and cohesive muddy beds, permanent maintenance dredging is required for safe navigation in these areas. Mud is a mixture of clays, silts, and fine sand with organic matter, the behavior of which is characterized as cohesive when it is dominated by a clay-size fraction of greater than 10–15%. In such cohesive and muddy beds, the non-Newtonian fluid mud formation, which is a high-concentration suspension of fine sediment, is also an essential factor in determining the transport and sedimentation process [1,2]. In order to reduce deposition and sedimentation problems in ports and navigation channels, some engineering solutions have been proposed by PIANC [3]. One of the proposed economical solutions and strategies in this report is “Keep Sediment Navigable”, which straddles the treatment and accommodation categories. Ships and vessels can navigate safely and efficiently in fluid mud, and this has led to measuring nautical depth as navigable depth in muddy beds. According to the PIANC Report [4], nautical depth is “the level where physical characteristics of the bottom reach a critical limit beyond which contact with a ship’s keel causes either damage or unacceptable effects on controllability and maneuverability.” Based on this, the navigable depth is the distance between the free surface of water and the nautical

bottom with a given suspension density as the reference parameter, typically in the range of 1100 to 1300 kg/m³ [1,3,5–8]. The nautical bottom approach can be implemented to reduce the amount of dredging and its costs in such ports. The two forms of the nautical bottom approach are the Passive and the Active Nautical Depth [3,9,10]. The Passive Nautical Depth is the most common approach which measures density and defines channel depth as the horizon at which density is a specified value, typically 1100 to 1300 kg/m³ [11,12]. The Active Nautical Depth approach is a more recent solution, involving deliberate agitation of mud to create an aerobic and stable suspension at a low density which prevents it from consolidating into a sediment bed [9,13].

In the past decades, extensive efforts have been made to employ both Passive and Active Nautical Depth approaches in ports and navigation channels to reduce dredging costs, including Emden, Germany; Zeebrugge, Belgium; Rotterdam and Delfzijl, the Netherlands; Cochin, India; etc. [8,13–17]. In order to determine the physical characteristics of the bottom and define the nautical bottom, some innovative approaches have been examined and proposed by many researchers. A comprehensive research project was carried out to define the nautical bottom approach in the harbor of Zeebrugge, Belgium, at Flanders Hydraulics Research and the Maritime Technology Division of Ghent University [18–21]. Moreover, some research projects have been carried out to investigate the nautical bottom approach in navigation channels in the United States [1,11]. The implementation of a nautical bottom approach in the Port of Santos, Brazil, was investigated, and a fluid mud layer with a thickness of a few centimeters to approximately 1 m was reported in this port as obtained from the acoustic and density profile measurements [22]. One of the most crucial factors in the nautical bottom approach affecting the dynamics and navigability of the bottom in ports and waterways is the rheological properties of fluid mud, which have been examined in recent decades. The rheological properties of mud and the effect of the physical, chemical, and mineralogical characteristics of sediment on viscosities and yield stress parameters were investigated in different areas such as the Krishna Godavari offshore basin to the east of India as well as the Chorfa dam region of Mascara, Algeria [23,24]. Moreover, in order to study cohesive sediment transport in West Lake, Hangzhou, China, the investigation of vertical stratification and the rheological properties of near-bed cohesive sediments were carried out by measuring rheological properties including apparent viscosity, shear stress, and yield stress; physical properties such as concentration, density, and particle size of the sediments in the study area were carried out as well [25]. The rheological properties of collected mud sediments from the Port of Hamburg, Germany, showed the relatively small yield stress and weak thixotropic behavior of the fluid mud layer in the study area. The combination of yield stress and density were used to define the nautical bottom definition in the Port of Hamburg, and an overview of the rheological properties of the mud and other affecting factors from different sources were investigated [26,27].

There are several ports over the Iranian bodies of water, such as Bushehr, Imam Khomeini, and Sajjafi in the Persian Gulf and the Anzali Port in the Caspian Sea, for which the nautical bottom approach can be assessed based on sediment conditions. Due to the deposition of fine sediments in these ports, specific practical considerations need to be taken into account to maintain enough depth in these ports and their access channels for safe navigation. The main objective of this study is to investigate the feasibility of implementing the nautical bottom approach to reduce and manage the high sedimentation and siltation in the Bushehr Port and its access channel. In this study, the essential characteristics and parameters of the sediment have been considered through a comprehensive sediment sampling in the field and complementary laboratory studies.

2. Materials and Methods

2.1. Study Area

The Bushehr Port is located in the Soltani Estuary in the Bushehr Peninsula on the coast of the Persian Gulf and it is one of the most important commercial ports in

southwestern Iran. The Bushehr Peninsula is surrounded by land and consists of shallow water areas confined by the Bushehr headland in the south and the Helleh River delta in the north (Figure 1). This delta has been formed by fluvial sediments, mostly coming from the Helleh River system and partly from other rivers located in the northern part of Bushehr Bay. A major part of the peninsula is considered shallow water areas and tidal flats with varying depths of less than 5 m. The only deep navigable area is the tidal channel of the Soltani Estuary, located in the northeastern part of the Bushehr Peninsula [28].

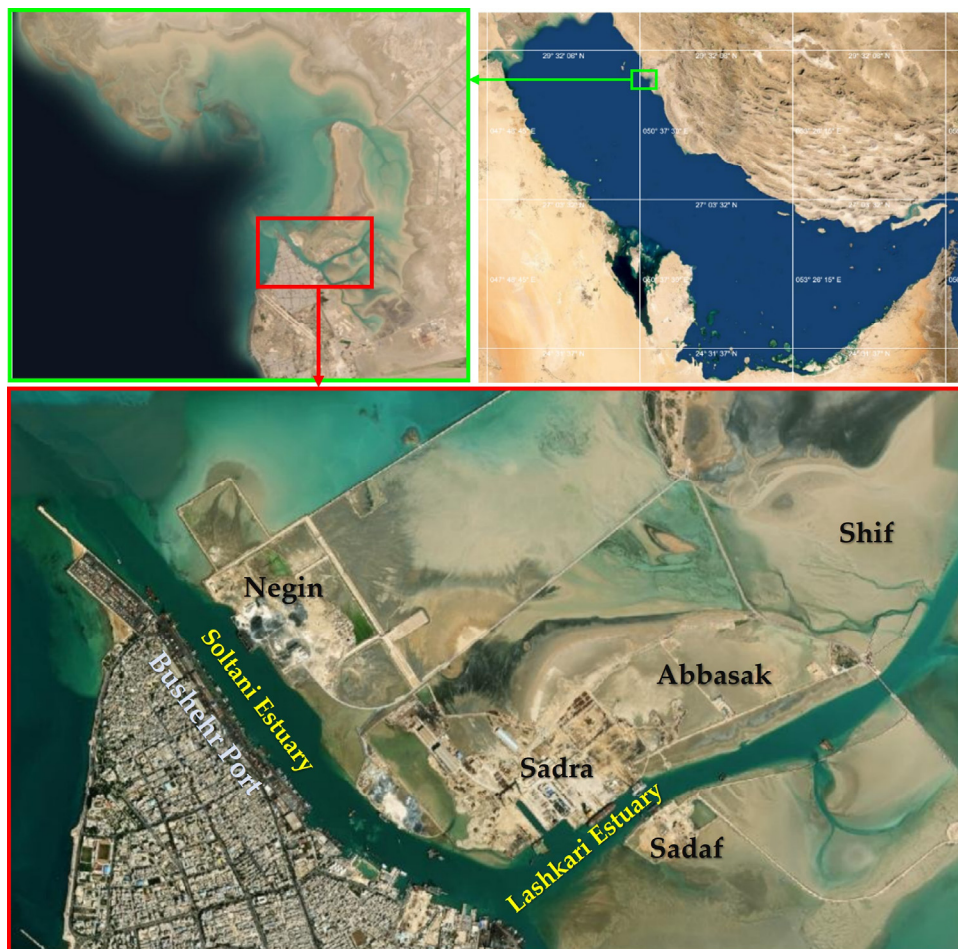


Figure 1. A view of Bushehr Peninsula (top) and the location of Bushehr Port (bottom).

The Bushehr Port access channel consists of two segments; the inner and outer channel, which are 3.2 and 9.3 km long, respectively (Figure 2). The inner channel has the same alignment as the Soltani Channel and is connected to the outer channel with a 100° bend. As the channel is located in a very shallow area, continuous deposition of fine sediments leads to deposition rates between 300,000 and 900,000 m^3/year (10–15 cm/year). A significant volume of annual maintenance dredging is necessary which is very costly for the port; hence, the continuous dredging of approximately 260,000 m^3/year is carried out in this port. Over the past three decades, the average deposition rate between two capital dredging works is between 500,000 and 700,000 m^3/year . Meanwhile, after the deepening of the access channel in 2007–2008, the depth of the inner and outer channels has increased to 10.3 and 10.8 m, respectively [29].

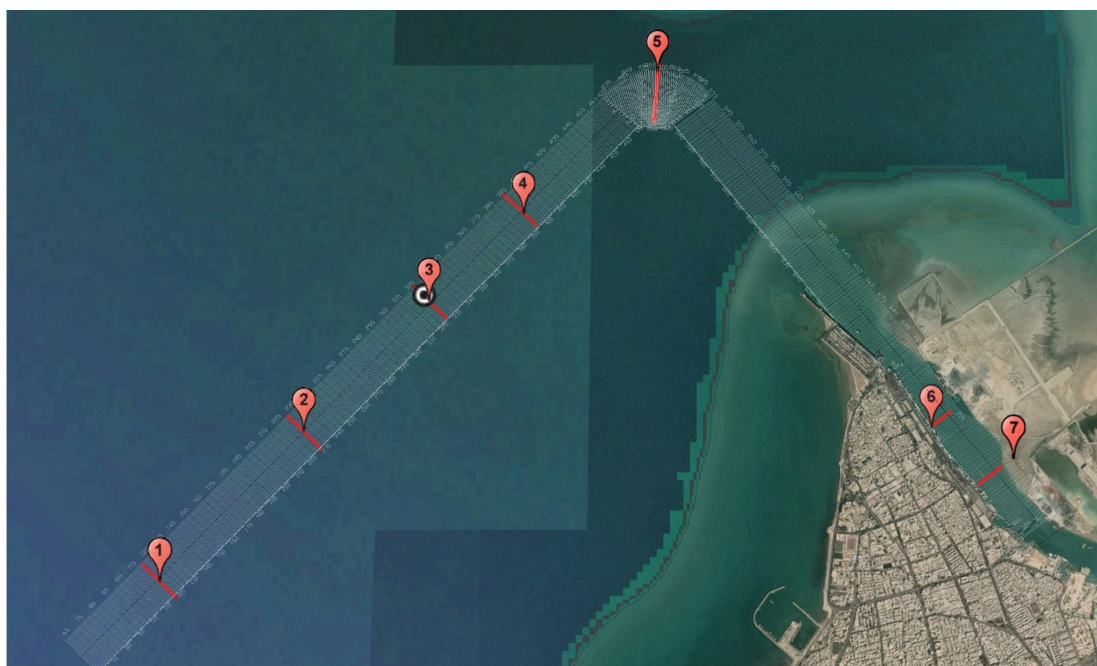


Figure 2. Locations of surface (7 points shown by numbered pin icons) and core (1 point shown by circle placemark icon) sediment sampling, and selected lines of hydrographic survey with dual-frequency echo sounder (7 transects shown by red line) along the access channel of Bushehr Port.

The field study was carried out to evaluate the fluid mud and sediment properties in the area. In order to investigate the presence of fluid mud and estimate the thickness of this layer, data from a hydrographic survey with a dual-frequency echo sounder were used. Moreover, the properties of the sediment in various locations in the port and its access channel were analyzed by collecting the surface and core sediment samples in selected locations and performing a series of laboratory experiments, including sediment grain-size analysis and grain-size distribution, analysis of the carbonate and organic matter content, rheometry, and consolidation and settling tests.

2.2. Hydrographic Survey

In order to estimate the fluid mud thickness in the study area, hydrographic surveys in the inner and outer channel were performed using a DESO30 dual-frequency echo sounder by Darya Tarsim Consulting Engineers. The dual-frequency echo sounder, operating with two transducers (one with a high frequency of 200 kHz, and the second with a low frequency of 30 kHz), was used to identify the in situ thickness of the fluid mud layer. High- and low-frequency echo sounders reflect at the mud–water interface (i.e., the lutocline), and the hard bottom or the consolidated mud layer, respectively [30,31]. In total, 888 transects with a distance of 20 m were chosen in the inner and outer channels to estimate the spatial variability of the fluid mud thickness in the study area (Figure 2).

2.3. Sediment Sampling

In order to investigate the characteristics of surface sediment and depth variations of sediment properties in the port and its access channel, 7 points for surface sampling and 1 point for core sampling were considered in the field survey (Figure 2). The selected transects in the location of sampling points are also depicted in Figure 2. Other details of sampling locations, including the coordinates and depths, are listed in Table 1. In this table, the listed depths are related to the depths measured during the collection of samples and those obtained from the latest available hydrographic survey data (relative to the chart datum). Surface samples were collected using the Van Veen grab sampler, and the core

sample was collected using a gravity corer featuring a detachable core tube with a length of 120 cm.

Table 1. Sediment sampling locations.

Sampling Point No.	Longitude	Latitude	In Situ Depth (m)	Depth Based on the Latest Hydrographic Survey Data (m, Relative to CD)
S1	50.75677	28.9774	−9.5	−9.4
S2	50.77087	28.9909	−8.5	−9.0
S3	50.78357	29.0030	−9.1	−8.0
S4	50.79344	29.0112	−8.0	−8.5
S5	50.80781	29.0252	−9.8	−7.6
S6	50.83674	28.9911	−8.0	−10.1
S7	50.84524	28.9883	−1.2	−1.0
C	50.7832	29.00332	−7.0	−8.3

2.4. Grain-Size Distribution

The primary purpose of this test is to derive the grain-size distribution and determine the grain-size fractions, including sand, silt, and clay of each sample, using the Laser Particle Sizer “analysette22” instrument at the Material and Energy Research Center (MERC). This instrument is a high-performance particle-size analysis system incorporating modes for measuring both dry and liquid samples in the range from 0.16 μm to 1160 μm according to the international standard ISO “Particle-size analysis—Laser diffraction methods” [32]. It uses the patented FRITSCH measuring principle with a convergent laser beam which allows a high resolution of up to 310 measurement channels. There are several systems of soil and sediment classification which are based on particle size or soil and sediment properties, such as the U.S. Department of Agriculture (USDA), International Society of Soil Science (ISSS), and the British Soil Classification System (BSCS), etc. A summary of the BSCS classes according to size is given in Table 2.

Table 2. Sediment grain-size range in the British Soil Classification System (BSCS).

Name and Class		Size Range (mm)	
Very coarse	Boulders	>200	
	Cobbles	60–200	
Coarse	Gravel (G)	Coarse	20–60
		Medium	6–20
		Fine	2–6
Fine	Sand (S)	Coarse	0.6–2.0
		Medium	0.2–0.6
		Fine	0.06–0.2
Fine	Silt (M)	Coarse	0.02–0.06
		Medium	0.006–0.02
		Fine	0.002–0.006
	Clay (C)	<0.002	

2.5. Carbonate and Organic Matter Content

X-ray fluorescence (XRF) spectroscopy analysis is one of the elemental and oxide analytical methods used to detect sediment elements. The XRF instrument is used for measuring the wavelength and the intensity of scattered X-ray fluorescence waves from different atoms in the sample which results in the detection of the content and amounts of the component materials. This test was performed in the Central Laboratory of Tehran University, using a Spectro Xepos instrument that simultaneously measures the percentage of the elements and their oxidation states for almost 80 elements.

Organic matter profoundly affects the physical, chemical, and biological properties of fine sediments. Some of the properties influenced by organic matter include sediment structure, compressibility, and shear strength [33]. In order to obtain the organic content, the laboratory instruction based on ASTM “Standard Test Methods for Moisture, Ash, and Organic Matter of Peat and Organic Soils” has been implemented [34]. The proposed testing procedure in this standard for the determination of the organic matter is based on the loss-on-ignition (LOI) method which involves the heated destruction of all organic matter in the sediment sample. A known weight of dry sediment sample is placed in an empty, clean, and dry pan, which is then heated to 440 ± 40 degrees Celsius overnight. The organic matter content is calculated by the following formula:

$$\text{OM} = (\text{MO}/\text{MD}) \times 100 \quad (1)$$

where MO is the mass of the organic matter ($=\text{MD}-\text{MA}$), MD is the mass of the dry sediment, and MA is the mass of the burned sediment.

2.6. Rheometry

The aim of the rheological tests is to investigate the changes in the deformation and fluids and quasi-solids flow behavior of the sediment samples under applied shear stress. This behavior can be investigated using both rotational (or static) and oscillatory (or dynamic) experiments. The rheological properties obtained from these tests indicate the behavior of materials in dynamic environments (such as currents and waves). In general, the procedures for performing rheometry are shown in Figure 3. Static tests involve the imposition of a step change in stress (or strain) and measurement of the subsequent strain (or stress) changes while the dynamic tests involve the application of harmonically oscillating stress (or strain). In both rotational and oscillatory tests, two procedures can be performed: (a) controlled shear rate or deformation (CSR–CSD) and (b) controlled shear stress rate (CSS).

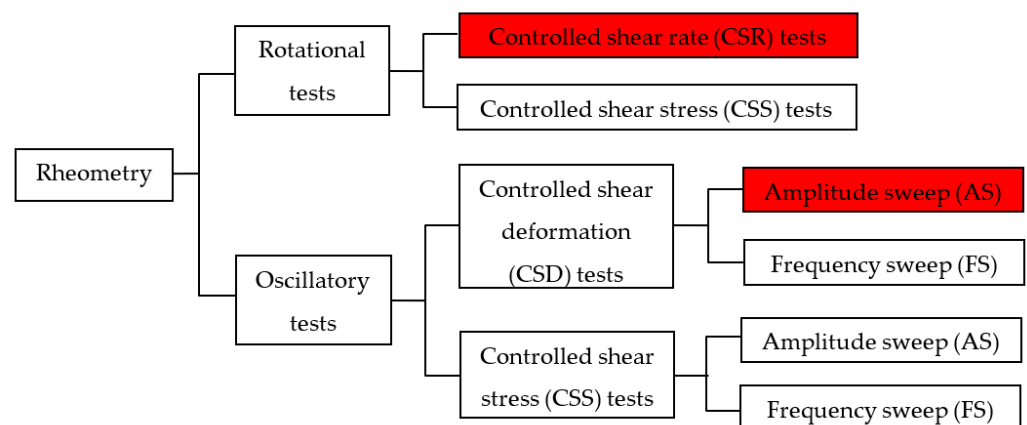


Figure 3. Rheometry methods (Colored areas indicate tests conducted in this study).

In order to study the rheological properties of the sediment samples, the rheometric tests were performed using the Anton Paar Physica MCR301 rheometer with the vane-in-cylinder geometry in the Material and Energy Research Center (MERC). In order to draw the rheogram and viscoplastic deformation curves in the CSR rotational test, a controlled shear rate ($d\gamma/dt$) in the range of 0.1 to $10 \text{ (s}^{-1}\text{)}$ is considered as a logarithmic input, and the recorded shear stress as an output. In the CSD oscillatory test, an amplitude sweep (AS) in the range of 0.01 to 100% is considered as a logarithmic input with a constant value of angular frequency of 10 rad/s , and the recorded values of storage and loss modulus as outputs. Both experiments were performed at a constant temperature of $21 \text{ }^\circ\text{C}$. To investigate the changes in rheological properties of sediment with time, the experiments

were performed in three steps: (I) after stirring the sample, (II) after two days of resting, and (III) after two weeks of resting.

In the rotational experiments with controlled shear rate (CSR), the output results are presented in the form of flow curves (shear stress versus shear rate). There are various curve fitting models for flow curves; the simplest and most commonly used is the Bingham model. The linear function of the Bingham model for flow curves with yield points is as follows:

$$\tau = \tau_B + \eta_B \dot{\gamma} \quad (2)$$

where τ is shear stress, $\dot{\gamma}$ is shear rate, τ_B is the Bingham yield stress (same as yield stress τ_y with index B to determine the Bingham model) as an axis intercept, and η_B is the Bingham viscosity derived from the slope of the curve. In the Casson model, curve fitting is performed using the square root function and expressed as follows:

$$\tau^{\frac{1}{2}} = \tau_{yC}^{\frac{1}{2}} + (\eta_C \dot{\gamma})^{\frac{1}{2}} \quad (3)$$

where τ_{yC} is the Casson yield point, and η_C is the Casson viscosity [35].

In order to investigate the changes in rheological properties of sediment samples, the water contents w , as well as the sediment densities and concentrations, are determined. The relationship between density ρ , solid fraction volume φ ($=C/\rho_s$) and concentration C is as follows [36]:

$$\rho = \rho_w(1 - \varphi) + \rho_s \varphi = \rho_w(1 - \varphi) + C \quad (4)$$

where ρ_w and ρ_s are the density of water and the grain density of sediment, respectively. The particle density is measured by pycnometer which is based on Archimedes law using alcohol as the filling liquid. The density and water content of samples are measured by the cylinder and oven drying the sediment samples, respectively. In this study, the density of water is 1025 kg/m^3 and the grain density of the sediment in the outer, bend, and inner segments of channel are 2617 , 2556 , and 2588 kg/m^3 , respectively.

2.7. Consolidation and Settling of Sediment

In this experiment, nine dry masses of sediment samples (i.e., 10, 30, 50, 70, 100, 150, 200, 250, and 300 g) were mixed in a cylinder with 1 L of water, and the cylinder was agitated by a mechanical shaking device. In the relaxation period, due to sedimentation and settling of the suspension sediment, the volume of settled sediment was observed and recorded in 5 steps (Initial state, and after 1, 4, 6, and 11 days). The solid volume fraction (also called volumetric concentration) is recorded as output in each step which is defined as the ratio of solid volume to total volume. One of the proposed relationships for determining the rate of decrease in the concentration of suspended sediments is the Krone relationship with the no-flow condition as follows [37]:

$$C(t) = C_0 e^{-\left(\frac{w_s}{H}\right)t} \quad (5)$$

where $C(t)$ is the concentration change over time, C_0 is the initial suspended sediment concentration, w_s is the fall velocity, H is the water column height, and t is the time.

3. Results

3.1. Depth Estimation from Dual-Frequency Echo Sounder

In both the inner and outer parts of the channel, a muddy bottom was observed, and two levels were distinguished. The thickness of the fluid mud layers varied between a few centimeters and approximately 1 m along the channel. Figure 4 shows the obtained digital depth profiles using the dual-frequency echo sounder (blue and cyan lines indicate the computed high- and low-frequency sounding depths, respectively) compared with the available bathymetry performed in 2010 (magenta line) in selected locations along the navigation channel. In the outer section of the channel, high sedimentation was observed.

The erosion pattern occurred in the inner section of the channel, and relative stability was observed in line No. S7.

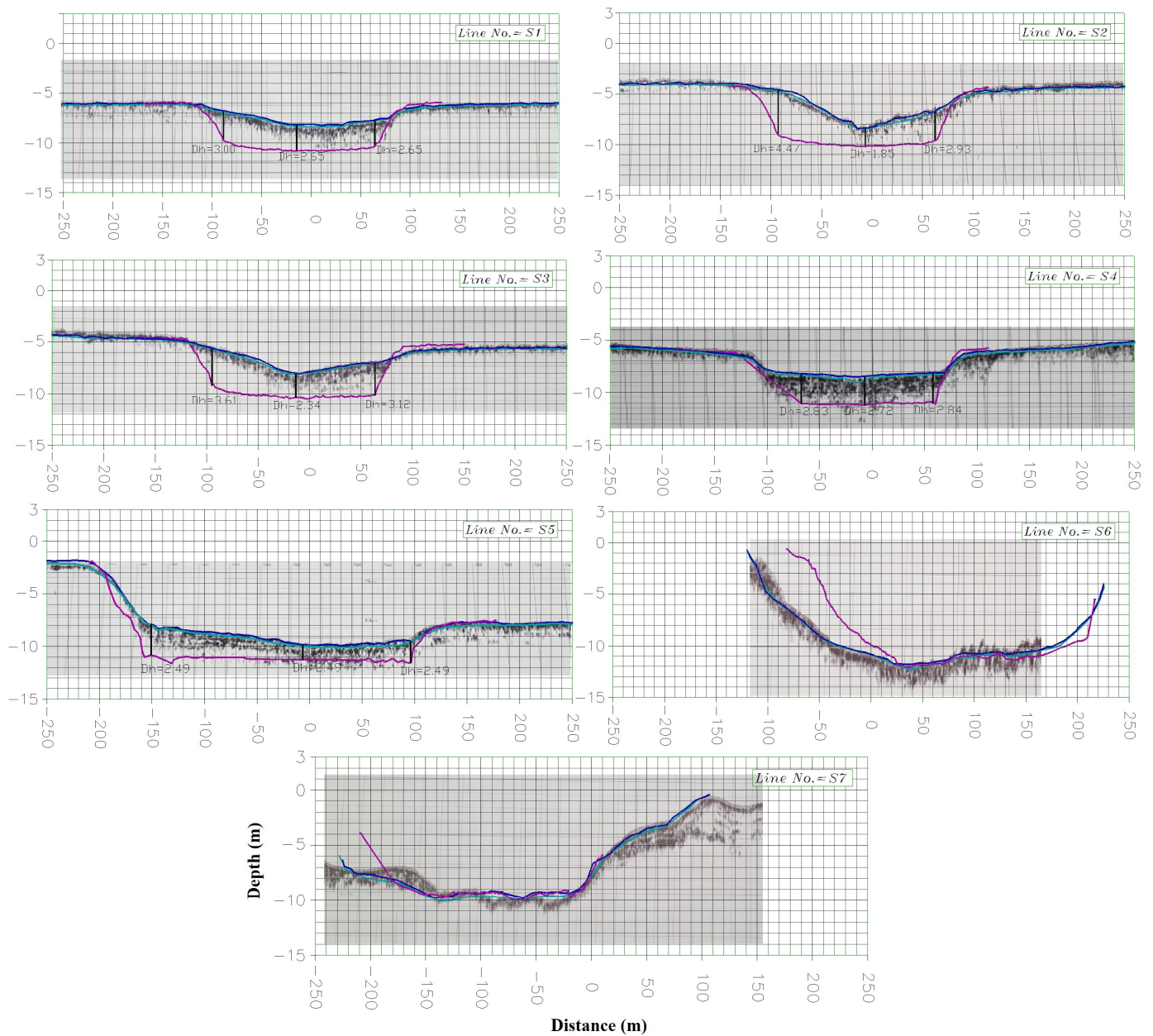


Figure 4. Digital depth profiles at the selected survey locations (7 transects; as depicted in Figure 2). The blue and cyan lines indicate the computed high- and low-frequency sounding depths, respectively, and the magenta line indicates the available bathymetric data in 2010.

3.2. Grain-Size Distribution Analysis

The British Soil Classification System (BSCS), presented in Table 2, has been used to classify sediment samples in this study. The particle-size distribution (i.e., sand-, silt-, and clay-size fractions), median particle size (D_{50}), and water content (w) of all the collected surface samples along the channel are listed in Table 3.

Table 3. Sediment grain-size analysis, median particle size, water content, and carbonate and organic matter content results.

Sample	w (%)	Clay	Silt	Sand	D ₅₀ (μm)	Carbonate Content	Organic Matter Content
S1	67%	26%	73%	1%	4.66	52.92%	0.25%
S2	60.23%	18%	77%	5%	8.51	57.23%	0.24%
S3	80.90%	23%	77%	-	5.22	56.3%	0.25%
S4	75.08%	30%	67%	3%	6.77	56.09%	0.28%
S5	59.85%	31%	69%	-	3.39	54.79%	0.29%
S6	99.35%	31%	69%	-	3.22	53.06%	0.27%
S7	37.45%	-	48%	52%	63.76	70.62%	0.31%

3.3. Carbonate and Organic Matter Content Estimation

Elemental and oxide analyses of sediments were performed using X-ray fluorescence spectroscopy (XRF). Table 3 shows the percentage of carbonate sediments extracted from the elemental and oxide analyses. Based on the loss-on-ignition (LOI) method and the aforementioned standard procedure for estimating organic matter, the obtained percentage of organic matter in the sediment samples is also listed in Table 3.

3.4. Rheological Properties of Sediment

In this section, the rheological parameters of sediments are presented according to two types of rotational experiments with controlled shear rate (CSR) and oscillatory experiments with controlled shear deformation (CSD) and amplitude sweep mode (AS). As mentioned, in order to investigate the changes in rheological behavior with time, the experiments were performed in three steps: (I) after stirring the sample, (II) after two days of resting, and (III) after two weeks of resting. An example of a rotational test output for the S4-I sample with a water content of 75.08% is shown in Figure 5. The fitted Bingham and Casson models are also shown in Figure 5. It is observed that the Bingham fitting model is relatively simple, so the Casson model is used as the flow curve fitting function for all sediment samples in this study. Furthermore, the Casson and some other rheological models have been proposed to fit the flow curve of cohesive sediment by many previous studies and it has been reported that nonlinear models would be in better agreement with data on soft muds [2,36]. Table 4 presents the water content, density, and concentration of sediment samples at each step. Table 5 presents the Casson yield point stress (τ_{yC} , Pa) and viscosity (η_C , Pa.s) for all samples. An example of the measured AS oscillatory test results is presented in Figure 6 for the sediment sample S5-I. In this figure, three zones listed as the linear viscoelastic range (LVR), yield zone (YZ), and liquid range (LR) are also shown. In terms of shear stress, the upper limit of this range is defined as the yield stress (τ_{yos}). The second significant stress in this diagram is at the intersection point of the two curves G' and G'' (in this crossover point $G' = G''$), which is called the flow-point stress (τ_f). Table 6 also presents the yield and flow-point stress values for all samples from the oscillatory test results. It is noteworthy that due to the non-cohesive behavior of sediment sample S7, it is not possible to measure some parameters for this sample (mentioned as N/A in the tables).

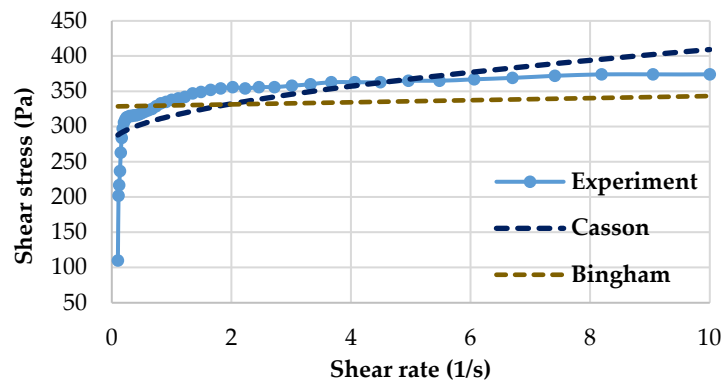


Figure 5. Flow curve for Sample S4-I with Casson and Bingham curve fitting models.

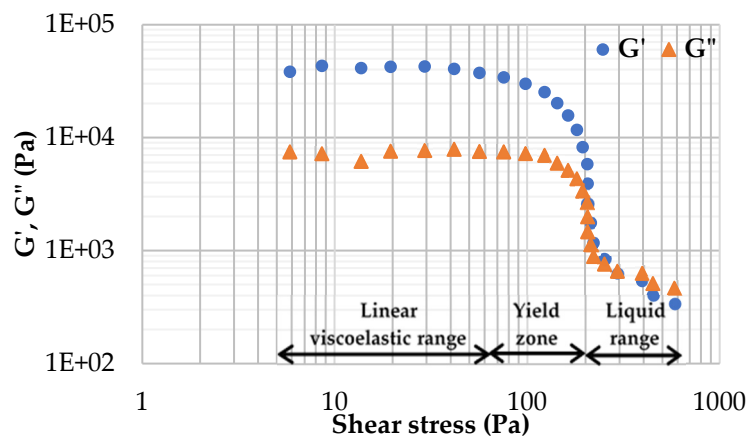


Figure 6. Oscillatory amplitude sweep test results for Sample S5-I.

Table 4. Water content, density, and sediment concentration in sediment samples for three steps.

Sample No.	(I) Stirring the Sample			(II) Two Days of Resting			(III) Two Weeks of Resting		
	<i>w</i> (%)	ρ (kg/m ³)	<i>C</i> (kg/m ³)	<i>w</i> (%)	ρ (kg/m ³)	<i>C</i> (kg/m ³)	<i>w</i> (%)	ρ (kg/m ³)	<i>C</i> (kg/m ³)
S1	67	1612.31	965.46	68.39	1604.72	952.98	68.83	1602.36	949.10
S2	60.23	1652.32	1031.22	61.63	1643.60	1016.90	62.60	1637.71	1007.20
S3	80.90	1544.32	853.69	81.62	1541.23	848.60	84.60	1528.8	828.17
S4	75.08	1558.03	889.90	68.66	1589.49	942.43	73.66	1564.68	901.01
S5	59.85	1639.25	1025.50	61.85	1627.20	1005.38	61.56	1628.92	1008.25
S6	99.35	1470.49	737.64	101.17	1464.73	728.11	99.93	1468.64	734.58
S7	37.45	1828.36	1330.20	34.92	1855.63	1375.36	N/A	N/A	N/A

Table 5. Casson yield stresses and viscosities for all samples for three steps.

Sample No.	(I) Stirring the Sample			(II) Two Days of Resting			(III) Two Weeks of Resting		
	<i>C</i> (kg/m ³)	τ_{yC} (Pa)	η_C (Pa.s)	<i>C</i> (kg/m ³)	τ_{yC} (Pa)	η_C (Pa.s)	<i>C</i> (kg/m ³)	τ_{yC} (Pa)	η_C (Pa.s)
S1	965.46	779.05	3.42	952.98	771.7	8.7	949.10	1057.27	4.47
S2	1031.22	507.63	3.56	1016.90	421.58	2.88	1007.20	702.61	4.02
S3	853.69	226.79	0.78	848.60	77.58	19.77	828.17	70.18	20.03
S4	889.90	275.77	1.32	942.43	72.36	18.92	901.01	223.76	9.87
S5	1025.50	1018.75	2.97	1005.38	1395.54	23.28	1008.25	1913.68	3.97
S6	737.64	317.58	1.52	728.11	205.51	12.16	734.58	324.5	5.25
S7	1330.20	N/A	N/A	1375.36	N/A	N/A	N/A	N/A	N/A

Table 6. Obtained yield and flow-point stress values from oscillatory test results for three steps.

Sample No.	(I) Stirring the Sample			(II) Two Days of Resting			(III) Two Weeks of Resting		
	C (kg/m ³)	τ_{yos} (Pa)	τ_f (Pa)	C (kg/m ³)	τ_{yos} (Pa)	τ_f (Pa)	C (kg/m ³)	τ_{yos} (Pa)	τ_f (Pa)
S1	965.46	19.5	187	952.98	59.9	164	949.10	73.1	181
S2	1031.22	24.3	96.8	1016.90	20.2	70.1	1007.20	41.8	108
S3	853.69	19.3	61.2	848.60	15.1	56.5	828.17	18.1	51.7
S4	889.90	17.1	67.6	942.43	20.1	66	901.01	24	74.9
S5	1025.50	75.5	206	1005.38	121	305	1008.25	123	271
S6	737.64	18.3	101	728.11	24.5	79.3	734.58	26.9	85.6
S7	1330.20	N/A	N/A	1375.36	N/A	N/A	N/A	N/A	N/A

3.5. Consolidation and Settling Analysis

As mentioned, this experiment was performed on two sediment samples (i.e., S2 and S5) with nine different mixtures of dry sediment and water in 5 steps (Initial state, and after 1, 4, 6, and 11 days). Figure 7 shows the temporal changes in the solid volume fraction of the sediment samples S2 and S5 in the consolidation and settling experiment.

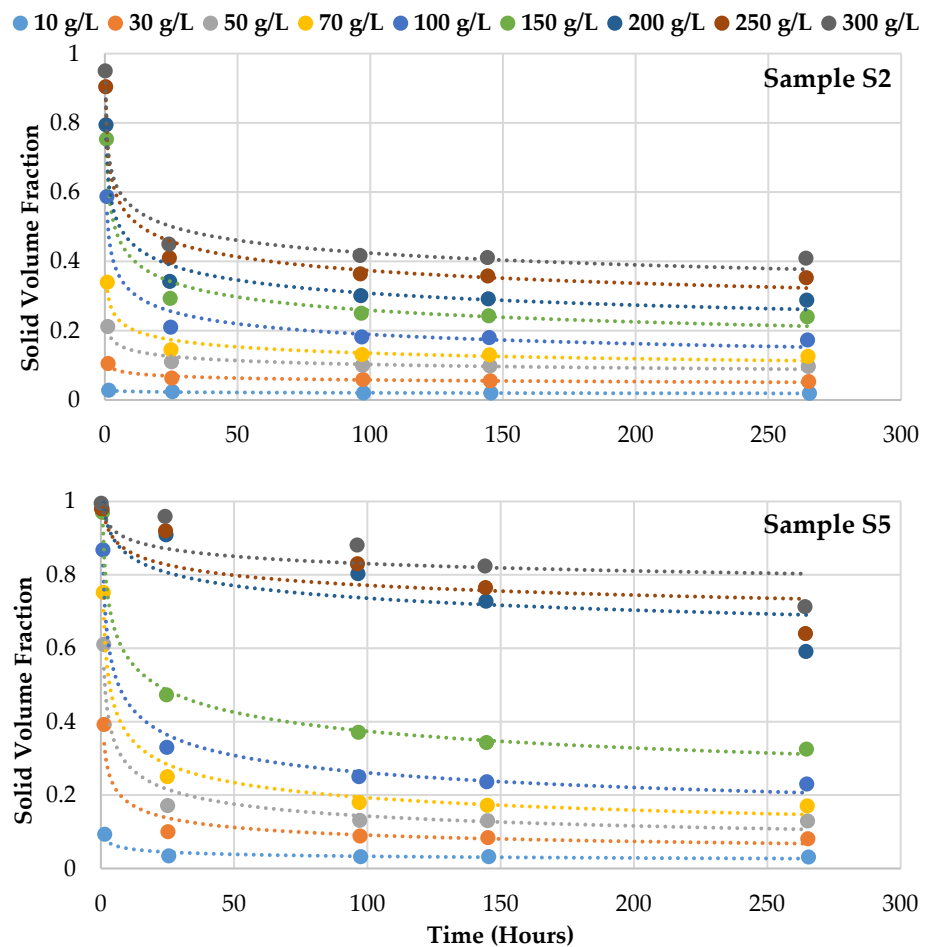
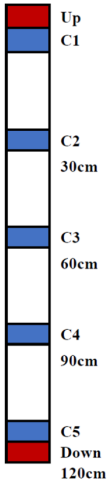


Figure 7. Temporal variations of the solid volume fractions for sediment Samples S2 and S5.

3.6. Core Sample Analysis

The height of the collected core sample in the desired position is 120 cm, and five samples in different depths have been selected according to the schematic drawing presented in Table 7. The experiments mentioned previously have been performed for each part of the core sample using the same protocols as the surface samples. Table 7 also presents the physical characteristics and rheological parameters obtained for each part of the core sample.

Table 7. Properties of sub-samples from the core sediment sample.

Core Sample	Sample No.	w (%)	Carbonate Content	Organic Content	D_{50} (μm)	Clay	Silt	Sand	Oscillatory Test	
									τ_{yos} (Pa)	τ_f (Pa)
	C1	8.44%	47.24%	0.19%	2.43	40%	60%	-	32.1	71.1
	C2	45.49%	47.05%	0.19%	55.11	5%	53%	42%	103	234
	C3	32.51%	50.85%	0.18%	29.95	10%	85%	5%	24	121
	C4	65.34%	49.12%	0.18%	3.37	32%	68%	-	38.1	107
	C5	66.08%	44.33%	0.18%	3.56	30%	70%	-	58.9	150

4. Discussion

4.1. Surface Sediment Sample Properties

The characteristics of surface sedimentary environments can be determined based on analyzing the sediment grain-size distribution within the study area. Figure 8 shows the distribution of the three grain-size fractions (i.e., sand, silt, and clay). As presented, the clay-size fraction in all samples, except sample S7, was between 20 and 30%. Since all samples (except sample S7) comprised clay-sized ($<2 \mu\text{m}$) and silt-sized ($<60 \mu\text{m}$) particles mixed with organic matter, they can be classified as cohesive sediments. The median size of cohesive samples in the study area was between 3.22 and 8.51 μm . In sample S7, the sand-size fraction was the most considerable (the median size is 63.76 μm), so it can be considered a non-cohesive sediment. The non-cohesive behavior of this sample was because of the reclamation work on the Negin Island development project. As previously mentioned, the rheological properties cannot be considered for this sample. Based on the provided general physical characteristics of the surface sediments in Table 3, the organic matter and the carbonate contents in the samples ranged from 0.24 to 0.31% and 52.9 to 57.2%, respectively. The high carbonate content in sample S7 was due to the presence of sand particles in this sample. The water content and the concentration of the sediment samples were lower than 100% and 1030 kg/m^3 , respectively.

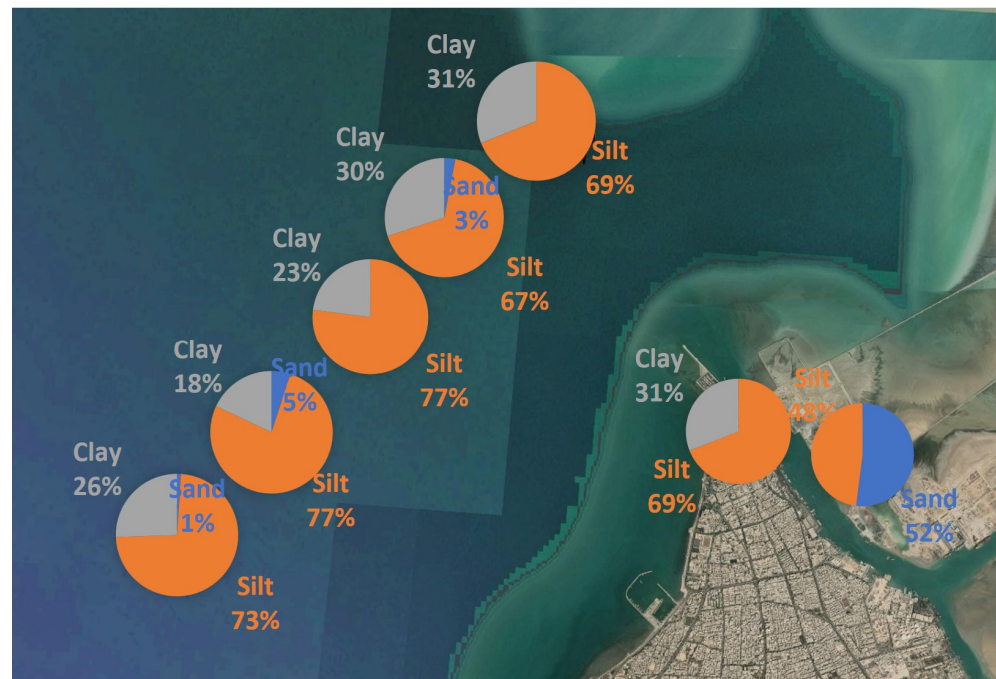


Figure 8. Distribution of grain-size fractions (sand, silt, and clay) in all surface sediment samples within the study area.

Concerning the rheological behavior of surface sediment, the relatively high values of stress were most likely related to using the Van Veen grab sampler and its heavier weight, which resulted in sampling at a greater depth than the fluid mud depth. Moreover, the yield stress values obtained from the rotational test were greater than the values from the oscillatory test, due to the different behaviors of the rotational and oscillatory experiments. As a result of the oscillating behavior of the wave and the tidal current, the oscillatory test outputs in the present study were more appropriate. Figure 9 illustrates the variation of obtained yield and flow-point stress values from the rotational and oscillatory tests versus the sediment concentration in all samples for three steps: (I) after stirring the sample, (II) after two days of resting, and (III) after two weeks of resting. The values of yield and flow-point stresses for different water contents indicated that the exponential function was a good fit for the results. Table 8 lists the fitted equations for obtained yield and flow-point stress values versus the sediment concentration in both rotational and oscillatory tests for the steps mentioned above. The rheological properties of the sediment samples are influenced by many factors, including water contents and concentration, temperature, organic matter content, the size and distribution of grains, and the type of clay mineral. Figure 10 shows the changes of different stresses of sediment samples with the water contents and grain-size fractions in each step. As it is observed, by neglecting the effect of small changes of organic matter and carbonate contents in all samples, the water contents and concentration, as well as the clay-size fractions, become the most important factors in rheological characteristics of sediment in the study area.

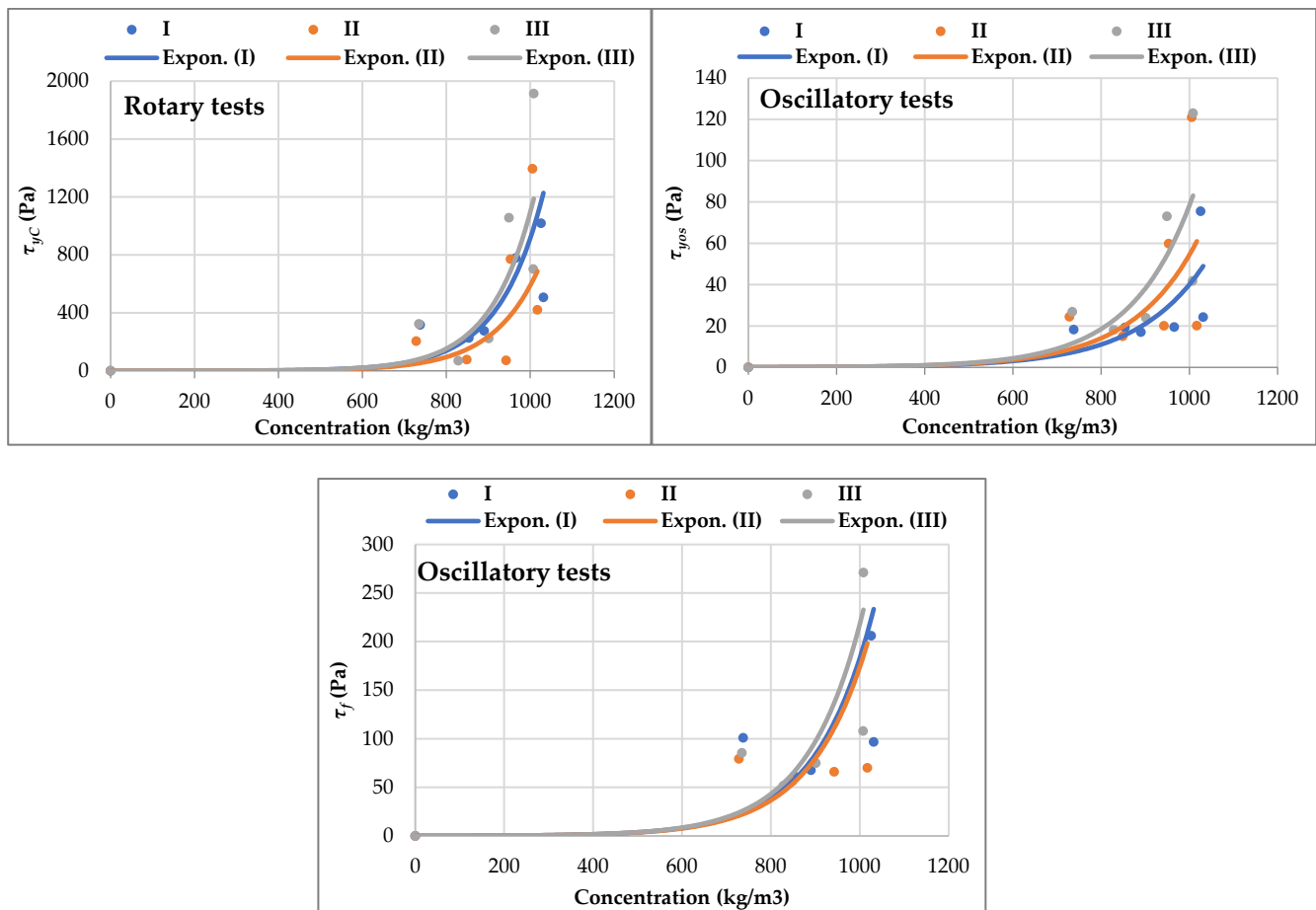


Figure 9. Yield and flow-point stress values versus sediment concentration in rotational and oscillatory tests.

Table 8. Relationship of yield and flow-point stress values versus sediment concentration in both rotational and oscillatory tests for three steps.

Tests/Steps	(I) Stirring the Sample	(II) Two Days of Resting	(III) Two Weeks of Resting
Rotary	$\tau_{yC} = 0.0737 e^{0.0094C}$	$\tau_{yC} = 0.0634 e^{0.0091C}$	$\tau_{yC} = 0.0582 e^{0.0098C}$
Oscillatory	$\tau_{yos} = 0.0639 e^{0.0064C}$ $\tau_f = 0.0748 e^{0.0078C}$	$\tau_{yos} = 0.0637 e^{0.0068C}$ $\tau_f = 0.0714 e^{0.0078C}$	$\tau_{yos} = 0.058 e^{0.0072C}$ $\tau_f = 0.0669 e^{0.0081C}$

4.2. Sediment Sample Properties over Depth

The core sample was divided into five parts, and the experiments as mentioned earlier were performed on each part. As presented in Table 7, the changes in the characteristics of sub-samples were significant. In the middle part, the sand-size fraction of samples was considerable (the sand-size fraction in sample C2 is 42%), which indicated that the sediments at this depth were transported under severe hydrodynamic conditions. The clay-size fraction at the lower depth and the top of the sample was approximately 30 to 40%. The obtained values of yield stress and flow-point stress from the oscillatory experiments increased in depth. The values of carbonate and organic matter contents did not change significantly in depth, and the carbonate content was between 44 and 52 percent, and organic matter was between approximately 0.18 and 0.19 percent.

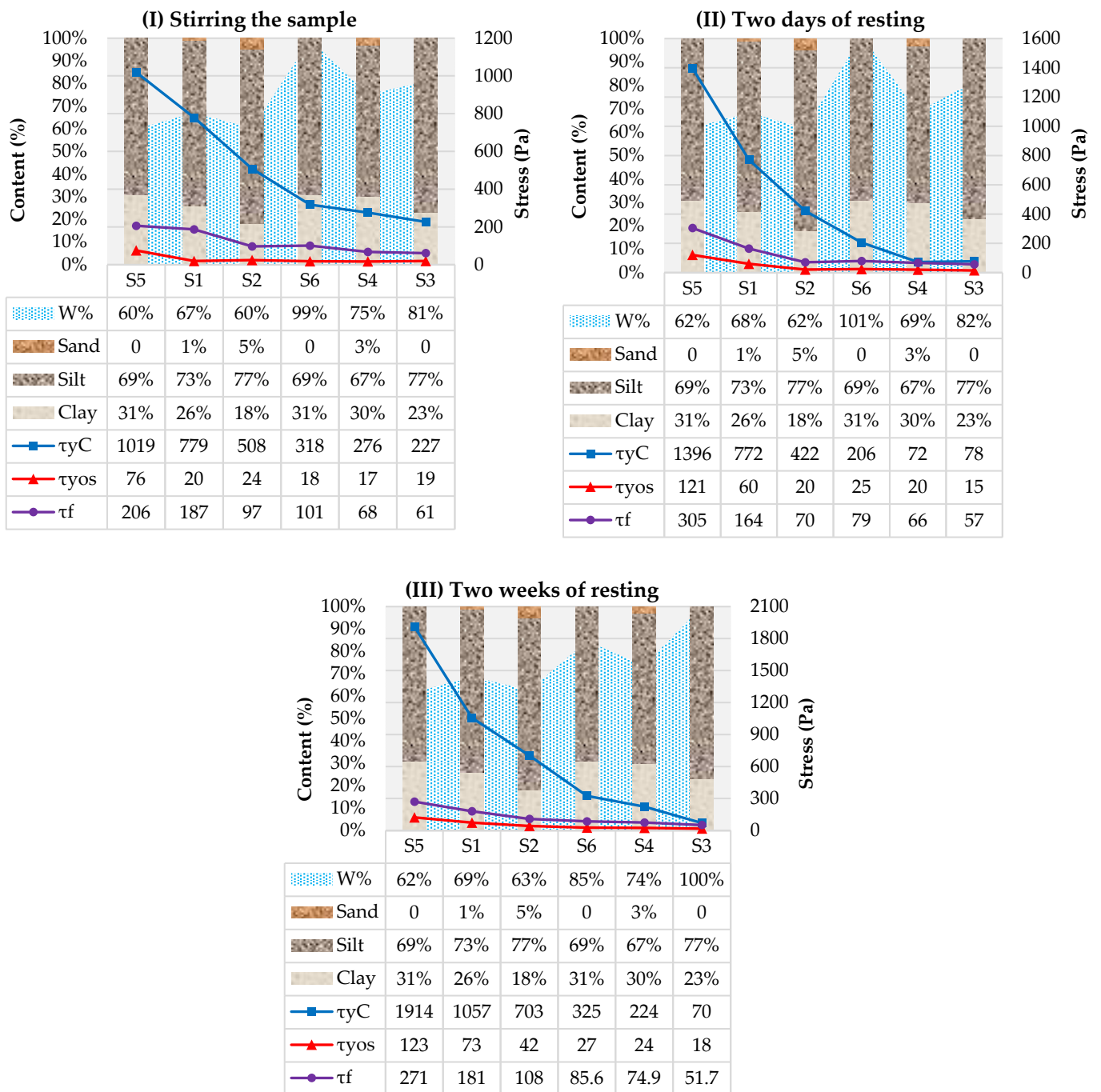


Figure 10. The rheological parameters of sediment samples with the water contents and grain-size fractions for three steps (I) Stirring the sample, (II) Two days of resting, (III) Two weeks of resting.

4.3. Seasonal Variations

In order to investigate the seasonal changes of characteristics, the sediment properties of two samples (i.e., No. S2 and S5) were compared in summer and autumn. Table 9 presents the yield and flow-point stress values of these samples in September and November. The spectroscopy analysis results for these two samples in September and November are also listed in Table 10. In November, the values of yield and flow-point stresses in both samples were larger than in September. According to the obtained results in November, the carbonate content was higher, and the silica content was lower than in September.

Table 9. Seasonal variations of yield and flow-point stress values obtained from oscillatory tests for samples No. S2 and S5.

Month	Sample No.	w (%)	τ_f (Pa)	τ_{yos} (Pa)
September	S2	58.83%	20.7	47
	S5	100.82%	10.8	58.8
November	S2	76.97%	31.7	61
	S5	84.36%	14.2	74.6

Table 10. Seasonal variations of elemental composition for samples No. S2 and S5.

Month	Sample No.	SiO ₂	CaO	Na ₂ O	P ₂ O ₅	Al ₂ O ₃	MgO	SO ₃	K ₂ O	Fe ₂ O ₃
September	S2	19.40	57.57	1.539	0.845	2.895	1.519	0.452	1.763	9.117
	S5	20.42	52.54	1.689	0.898	3.469	1.865	0.644	2.55	12.66
November	S2	18.34	59.73	1.294	1.056	2.906	1.557	0.37	2.008	11.72
	S5	20.15	55.50	1.397	0.837	3.456	1.834	0.436	2.301	11.07

5. Conclusions

Due to the presence of fine-grained and cohesive muddy deposits in the Bushehr Peninsula, special arrangements need to be considered to ensure that the Bushehr Port and its access channel are accessible and safe for navigation. In order to reduce the sedimentation and siltation and the consequent need for dredging in this port, the implementation of the nautical bottom approach was proposed. To assess the feasibility of nautical bottom approach in this port, the physical characteristics of the bed and the in situ properties of the fluid mud layer, which play important roles in the nautical bottom definition, were investigated in this study. A set of comprehensive laboratory experiments were carried out on the collected samples from different parts of the channel, including surface and core samples. The sediment characteristics were traced by grain-size composition, distribution pattern, water content ratio and concentration, carbonate and organic matter contents, rheological criteria, and consolidation and settling analysis. The sediment-size distribution showed that most sediment in the study area consisted predominantly of fine-grained particles, including silt and clay. The results of the core sample showed that changes in sediment characteristics such as water content and clay-, silt-, and sand-size fractions in depth were significant.

The four criteria for determining the nautical bottom in PIANC report No. 121 are echo sounding, rheology-related criteria, ship behavior, and mud density level. Based on the dual-frequency echo sounding data and the obtained high- and low-frequency echo sounder profiles, a fluid mud layer with a thickness of up to 1 m was detected in the channel. Comparing the depth profiles in different locations indicated an erosion pattern in the inner section and a sedimentation pattern in the outer section of channel. Due to the uncertainty of depth observation by acoustic echo sounding, specifically in a muddy environment, and in order to establish the location of the top of the fluid mud layer and the bed for an accurate definition of the nautical bottom, it is recommended that the in situ density surveys be conducted within the port. In terms of rheology-related criteria, both rotational and oscillatory tests were performed in this study. Many practical studies indicate that the yield stress values between 70 and 100 Pa with corresponding density values varying from 1100 to 1300 kg/m³ can be employed for a nautical bottom assessment. In the present study, the obtained values of yield stresses from oscillatory test results vary from 17 to 123 Pa. Based on comparing the obtained criteria for the nautical bottom in this study, it is concluded that a nautical bottom with potentially navigable layers of up to 1 m can be practically implemented to this port and its access channel.

Author Contributions: Conceptualization, F.S., S.A.H. and M.S.; methodology, F.S. and S.A.H.; formal analysis, F.S.; investigation, F.S., S.A.H. and M.S.; resources, M.S.; writing—original draft preparation, F.S.; writing—review and editing, S.A.H. and M.S.; visualization, F.S.; supervision, M.S. All authors have read and agreed to the published version of the manuscript.

Funding: This research received no external funding.

Institutional Review Board Statement: Not applicable.

Informed Consent Statement: Not applicable.

Data Availability Statement: The data presented in this study are available on request from the corresponding author.

Acknowledgments: This research project ‘Implementation of Passive/Active Nautical Depth in the Port of Bushehr’ was in the frame of the feasibility study of Minimizing Harbor Siltation, by Ports and Maritime Organization of Iran. The authors are especially thankful to Mohammad Hossein Nemati, Head of Coastal Engineering Department, Ports and Maritime Organization of Iran and Robert Kirby, marine geologist, sedimentologist, and co-inventor of Passive Nautical Depth at SEMASO B.V. Sediment Management Solutions, as well as colleagues at Darya Negar Pars Consulting Engineers and Darya Tarsim Consulting Engineers for their valuable contributions to this study.

Conflicts of Interest: The authors declare no conflict of interest.

References

- McAnally, W.H.; Kirby, R.; Hodge, S.H.; Welp, T.L.; Greiser, N.; Shrestha, P.; McGowan, D.; Turnipseed, P. Nautical Depth for U.S. Navigable Waterways: A Review. *J. Waterw. Port Coast. Ocean Eng.* **2016**, *142*, 04015014. [\[CrossRef\]](#)
- Mehta, A.J.; Samsami, F.; Khare, Y.P.; Sahin, C. Fluid Mud Properties in Nautical Depth Estimation. *J. Waterw. Port Coast. Ocean Eng.* **2014**, *140*, 210–222. [\[CrossRef\]](#)
- PIANC. *Minimising Harbour Siltation*; MarCom Working Group 102 (Rep. No. 102); PIANC (World Association for Waterborne Transport Infrastructure): Brussels, Belgium, 2008.
- PIANC. *Approach Channels—A Guide for Design*; MarCom Working Group 30 (Joint PIANC-IAPH Report); PIANC (World Association for Waterborne Transport Infrastructure): Brussels, Belgium, 1997.
- Kirby, R.; Parker, W.R. Seabed density measurements related to echosounder records. *Dock Harb. Auth.* **1974**, *54*, 423–424.
- Kirby, R.; Parker, W.R.; van Oostrum, W.H.A. Definition of the seabed in navigation routes through mud areas. *Int. Hydrogr. Rev.* **1980**, *57*, 107–117.
- Vantorre, M. Ship behaviour and control in muddy areas: State of the art, manoeuvring and control of marine craft. In *Proceedings of the 3rd International Conference on Manoeuvring and Control of Marine Craft, Southampton, UK, 14–17 July 1992*; Roberts, G.N., Pourzanjani, M.M.A., Eds.; 1994; pp. 59–74.
- Vantorre, M.; Laforce, E.; Delefortrie, G. A novel methodology for revision of the nautical bottom. In *Seminar: Flanders, a Maritime Region of Knowledge (MAREDFlow)*; Peeters, Y., Fockedeij, N., Seys, J., Mees, J., Eds.; Vlaams Instituut voor de Zee (VLIZ): Ostend, Belgium, 2006; pp. 15–34.
- Kirby, R.; Wurpts, R.; Greiser, N. Chapter 1 Emerging Concepts for Managing Fine Cohesive Sediment. In *Sediment and Ecohydraulics—INTERCOH 2005*; Elsevier: Amsterdam, The Netherlands, 2008; pp. 1–15. [\[CrossRef\]](#)
- Johnson, H.N.; McAnally, W.H.; Ortega-Achury, S. *Sedimentation Management Alternatives for the Port of Pascagoula*; Mississippi State University: Starkville, MS, USA, 2010.
- NRC (National Research Council). *Criteria for the Depths of Dredged Navigational Channels*; National Academies Press: Washington, DC, USA, 1983. [\[CrossRef\]](#)
- Xu, J.; Yuan, J. Study on the possibility of occurrence of fluid mud in the Yangtze deep waterway. In *Proceedings of the International Conference on Estuaries and Coasts, Hangzhou, China, 9–11 November 2003*; pp. 516–520.
- Wurpts, R.; Torn, P. 15 years experience with fluid mud: Definition of the nautical bottom with rheological parameters. *Terra et Aqua* **2005**, *99*, 22–32.
- Delefortrie, G.; Vantorre, M. The Nautical Bottom Concept in the Harbour of Zeebrugge. In *Proceedings of the 31st PIANC Congress, Estoril, Portugal, 14–18 May 2006*.
- Kirichek, A.; Chassagne, C.; Winterwerp, H.; Vellinga, T. How navigable are fluid mud layers? *Terra et Aqua* **2018**, *151*, 6–18.
- Verwilligen, J.; Vantorre, M.; Delefortrie, G.; Kamphuis, J.; Meinsma, R.; van der Made, K.J. Manoeuvrability in proximity of nautical bottom in the harbour of Delfzijl. In *Proceedings of the 33rd PIANC World Congress, San Francisco, CA, USA, 1–5 June 2014*.
- Ferket, B.; Heredia Gomez, M.; Rocabado, I.; De Sutter, R.; Van Hoestenbergh, T.; Kwee, J.; Werner, C.; Verwilligen, J.; Vos, S.; Vantorre, M.; et al. Assessment of siltation processes and implementation of nautical depth in the Port of Cochin, India. In *Proceedings of the CEDA Dredging days, Rotterdam, The Netherlands, 9–10 November 2017*.

18. Delefortrie, G.; Vantorre, M.; Eloot, K. Modelling Navigation in Muddy Areas through Captive Model Tests. *J. Mar. Sci. Technol.* **2005**, *10*, 188–202. [[CrossRef](#)]
19. Delefortrie, G.; Vantorre, M. Effects of a muddy bottom on the straight-line stability. In Proceedings of the 7th IFAC Conference on Manoeuvring and Control of Marine Craft, Lisbon, Portugal, 20–22 September 2006.
20. Delefortrie, G.; Vantorre, M.; Verzhbitskaya, E.; Seynaeve, K. Evaluation of Safety of Navigation in Muddy Areas through Real-Time Maneuvering Simulation. *J. Waterw. Port Coast. Ocean Eng.* **2007**, *133*, 125–135. [[CrossRef](#)]
21. Vantorre, M.; Eloot, K.; Delefortrie, G.; Lataire, E.; Candries, M.; Verwilligen, J. Maneuvering in Shallow and Confined Water. *Encycl. Mar. Offshore Eng.* **2017**, 1–17. [[CrossRef](#)]
22. Carneiro, J.C.; Fonseca, D.L.; Vinzon, S.B.; Gallo, M.N. Strategies for Measuring Fluid Mud Layers and Their Rheological Properties in Ports. *J. Waterw. Port Coast. Ocean Eng.* **2017**, *143*, 04017008. [[CrossRef](#)]
23. Chandrasekharan Nair, V.; Prasad, S.K.; Sangwai, J.S. Characterization and Rheology of Krishna-Godavari Basin Sediments. *Mar. Pet. Geol.* **2019**, *110*, 275–286. [[CrossRef](#)]
24. Messaoudi, A.; Bouzit, M.; Boualla, N. Physical and Rheological Properties of the Chorfa Dam Mud: Dependency on Solids Concentration. *Appl. Water Sci.* **2018**, *8*, 178. [[CrossRef](#)]
25. Yang, W.; Yu, M.; Yu, G. Stratification and Rheological Properties of Near-Bed Cohesive Sediments in West Lake, Hangzhou, China. *J. Coast. Res.* **2018**, *341*, 185–192. [[CrossRef](#)]
26. Shakeel, A.; Kirichek, A.; Chassagne, C. Rheological Analysis of Mud from Port of Hamburg, Germany. *J. Soils Sediments* **2020**, *20*, 2553–2562. [[CrossRef](#)]
27. Shakeel, A.; Chassagne, C.; Bornholdt, J.; Ohle, N.; Kirichek, A. From Fundamentals to Implementation of Yield Stress for Nautical Bottom: Case Study of the Port of Hamburg. *Ocean Eng.* **2022**, *266*, 112772. [[CrossRef](#)]
28. JWERC. *Monitoring and Modeling Study of Some Coastal Parts of Sistan and Baluchestan and Bushehr Provinces—Phase III*; PMO: Tehran, Iran, 2011.
29. Oceans Research Co. *Investigation of Sedimentation Pattern in the Bushehr Port after Its Development Project*; PMO: Tehran, Iran, 2020.
30. Carneiro, J.C.; Gallo, M.N.; Vinzón, S.B. Detection of Fluid Mud Layers Using Tuning Fork, Dual-Frequency Echo Sounder, and Chirp Sub-Bottom Measurements. *Ocean Dyn.* **2020**, *70*, 573–590. [[CrossRef](#)]
31. Kirichek, A.; Rutgers, R. Monitoring of settling and consolidation of mud after water injection dredging in the Calandkanaal. *Terra et Aqua* **2020**, *160*, 16–26.
32. *ISO 13320; Particle Size Analysis—Laser Diffraction Methods*. ISO 13320 (International Organization for Standardization): Geneva, Switzerland, 2020.
33. Deng, Z.; Huang, D.; He, Q.; Chassagne, C. Review of the Action of Organic Matter on Mineral Sediment Flocculation. *Front. Earth Sci.* **2022**, *10*, 965919. [[CrossRef](#)]
34. *ASTM D2974-20E01; Standard Test Methods for Determining the Water (Moisture) Content, Ash Content, and Organic Material of Peat and Other Organic Soils*. ASTM (American Society for Testing and Materials): West Conshohocken, PA, USA, 2014. [[CrossRef](#)]
35. Mezger, T.G. *The Rheology Handbook: For Users of Rotational and Oscillatory Rheometers*; Vincentz Network, Corp.: Hannover, Germany, 2014.
36. PIANC. *Harbour Approach Channels Design Guidelines*; MarCom Working Group 121 (Rep. No. 121); PIANC (World Association for Waterborne Transport Infrastructure): Brussels, Belgium, 2014.
37. Peixoto, R.S.; Rosman, P.C.C.; Vinzon, S.B. A Morphodynamic Model for Cohesive Sediments Transport. *Braz. J. Water Resour.* **2017**, *22*, e57. [[CrossRef](#)]